SCIENCE CHINA
Chemistry

•ARTICLES•

February 2024 Vol.67 No.2: 551–557
https://doi.org/10.1007/s11426-023-1754-5

C2-phenyl-substituted benzimidazolium-based covalent organic framework as efficient catalyst for CO_2 conversion without solvents, metals, and cocatalysts

Zhenzhen Wu[1], Jing Wang[2], Lili Liu[2], Shang Guo[1*], Juan Li[2*] & Xianming Zhang[3*]

[1]*Shanxi Institute for Functional Food, Shanxi Agricultural University, Taiyuan 030031, China;*
[2]*Institute of Crystalline Materials, Shanxi University, Taiyuan 030006, China;*
[3]*Key Laboratory of Interface Science and Engineering in Advanced Materials, College of Chemistry, Taiyuan University of Technology, Taiyuan 030024, China*

Received May 26, 2023; accepted August 14, 2023; published online October 30, 2023

Covalent organic frameworks (COFs) are a potential platform for carbon dioxide (CO_2) conversion owing to their periodic permanent porosity, adjustable structure, and chemical stability. For good catalytic performance in CO_2 conversion, collaborative multifunctions should be strategically integrated into the catalytic system design and construction. In this study, a four-in-one high-efficiency catalyst was synthesized and tested for CO_2 cycloaddition to form cyclic carbonate. The obtained Tp-MPB-Br-COF had a high nitrogen content, which enhanced its CO_2 affinity through substantial Lewis acid-base or dipole-quadrupole interactions; moreover, the acid (protons transferring from oxygen (–OH) to nitrogen (–NH)), hydrogen bond donor (hydroxyl group), and Br^- (nucleophile group) served as three active sites, further improving the catalyst activity. These results provide a basis for designing efficient and stable CO_2-conversion catalysts.

covalent organic framework, C2-phenyl-substituted, benzimidazolium, CO_2 conversion, four-in-one catalyst

Citation: Wu Z, Wang J, Liu L, Guo S, Li J, Zhang X. C2-phenyl-substituted benzimidazolium-based covalent organic framework as efficient catalyst for CO_2 conversion without solvents, metals, and cocatalysts. *Sci China Chem*, 2024, 67: 551–557, https://doi.org/10.1007/s11426-023-1754-5

1 Introduction

Massive emissions of the greenhouse gas carbon dioxide (CO_2) have led to global warming and glacier melting, thus attracting extensive research attention [1–3]. CO_2 fixation, *i.e.*, the catalytic conversion of CO_2 into value-added chemicals, is an attractive sustainable approach that has become a research hotspot compared with CO_2 capture and sequestration; in particular, the chemical fixation of CO_2 into cyclic carbonate is an effective and atomically economical approach for C1 resource utilization [4–12]. So far, researchers have explored various catalytic systems for CO_2 cycloaddition, including homogeneous and heterogeneous catalytic systems [13–21]. However, a rational construction of efficient heterogeneous catalytic systems for CO_2 conversion is urgently required.

Crystalline porous materials (CPMs) exhibit good applicability in gas adsorption [22–25] and catalysis [26–32] owing to their predictable structures. Covalent organic frameworks (COFs) are a new type of CPMs and comprise organic building blocks linked by reversible covalent bonds. COFs offer excellent performance, clear and predictable organic microporous/mesoporous architecture, good physical and chemical stability, a modifiable porous surface, and designable structure/properties [33–42]. However, as heterogeneous catalysts for the cycloaddition of epoxides with CO_2, most COFs exhibit low catalytic efficiency or require

*Corresponding authors (email: zhangxm@dns.sxnu.edu.cn; lj0511@sxu.edu.cn; gs0351@sohu.com)

cocatalysts [11,43–46]. Therefore, the synthesis of novel high-capacity COF catalysts remains a major challenge associated with CO_2 conversion.

Ionic liquids are organic salts comprising specific cations and anions and are widely used as CO_2-conversion catalysts [47]. However, their fluidity hinders product purification and recovery. Their other disadvantages include high viscosity and low diffusivity, resulting in tedious operating procedures and high costs. A possible solution is restricting the stable thin layers of ionic liquids in highly porous substrates [48–50]. The recovery performance of the resulting hybrid material has been doubted owing to the weak interactions between the encapsulated ionic liquid and porous matrix; moreover, accurately controlling the matching amount and spatial position in solid space is considerably challenging [2,45,51,52]. Thus, porous materials with active ionic groups offer an alternative for designing highly selective catalysts.

Herein, we synthesized a neutral imine COF (Tp-MPB-COF) modified by a C2-phenyl-substituted benzimidazole group. By ionizing its skeleton, we obtained an ionic COF (Tp-MPB-Br-COF) as a highly selective catalyst. First, the modularized synthesis strategy was used to selectively and uniformly embed the nitrogen-rich groups into the framework; the CO_2-philic nature of various nitrogen-rich groups, such as amines, imidazoles, carbazoles, and triazines, can be increased through significant Lewis acid-base or dipole-quadrupole interactions [53]. Second, the ionized COF structure exhibited tautomerism and acidity *via* proton transfer from oxygen (–OH) to nitrogen (–NH). Moreover, the hydrogen bond donor (hydroxyl group) and Br^- (nucleophile group) improved the catalytic activity with respect to CO_2 cycloaddition. Overall, we obtained a four-in-one high-efficiency catalyst for CO_2 conversion.

2 Results and discussion

Tp-MPB-COF was synthesized using C2-phenyl-substituted benzimidazole through the route shown in Scheme 1. MPB (0.36 mmol) and Tp (0.24 mmol) acted as a linker and knot, respectively, in the presence of 6-M acetic acid (0.3 mL) using *N*,*N*-dimethylacetamide/mesitylene (3 mL) as the solvent; the containing tubes were vacuum sealed and heated at 120 °C for 3 days.

The X-ray diffraction (XRD) patterns of Tp-MPB-COF exhibited an intense peak at 2θ = 2.86°, corresponding to (100) plane reflections (Figure 1b, structural simulations in Figure S1, and the atomistic coordinates of AA-stacking Tp-MPB-COF were summarized in Table S1, Supporting Information online). The Brunauer-Emmett-Teller (BET) surface area of Tp-MPB-COF was found to be 558.6 $m^2 g^{-1}$ (Figure 1c, Figure S2, and Table S2). The Fourier-transform infrared (FTIR) spectrum exhibited a strong peak at 1,587 cm^{-1}, attributed to the stretching of the keto form (Figure 1d). The Tp-MPB-COF isolation in the keto form was confirmed *via* solid-state ^{13}C nuclear magnetic resonance (NMR) analysis, which showed the carbonyl carbon signal at 184 ppm (Figure 1e). The powder XRD, X-ray photoelectron spectroscopy (XPS), and electron microscopy technology were used to investigate the stability of Tp-MPB-COF in solvents; Tp-MPB-COF (20 mg) was separately immersed in H_2O (10 mL), 9-N HCl, 9-N NaOH, and tetrahydrofuran (THF) for 7 days (Figures S3–S10), indicating remarkable stability.

Tp-MPB-Br-COF was prepared (see Supporting Information online) by ionizing Tp-MPB-COF with bromopropane (compared with various nucleophiles, bromopropane was selected as the preferred nucleophile, Figure S11). It exhibited an XRD pattern similar to that of Tp-MPB-COF, suggesting that the COF crystal framework was retained (Figure 1b, structural simulations in Figure S12, the atomistic coordinates of AA-stacking Tp-MPB-Br-COF were summarized in Table S2). However, the XRD peak intensity decreased, probably because charge interaction might have caused the destruction of crystal structure [54].

Nitrogen sorption measurements were conducted to verify the pore accessibility after ionization. Tp-MPB-Br-COF exhibited an isotherm similar to that of Tp-MPB-COF, while the BET surface area decreased to 382.9 $m^2 g^{-1}$ (Figure 1c, Figure S13, Table S2). We attribute this BET surface area reduction to the incorporation of larger substituents in the pore walls as well as the degradation of the crystal skeleton. Tp-MPB-Br-COF has also underwent the same stability verification in solvents as that of Tp-MPB-COF (Figures S14–S22), and it also demonstrated excellent stability.

After bromination, new peaks appeared at 3,035, 2,958, and 2,928 cm^{-1} in the FTIR spectra, indicating the presence of bromopropane. The peaks observed at 1,352 and 778 cm^{-1} were assigned to the vibration of imidazolium cations [55,56], confirming the existence of quaternary ammonium groups in the Tp-MPB-Br-COF structure.

Solid-state ^{13}C NMR was performed to analyze the structural composition of Tp-MPB-Br-COF (Figure 1e). The new peaks detected at 25, 21, and 11 ppm were ascribed to the propyl group in bromopropane, consistent with the FTIR results. This further indicates that the imidazole group underwent nucleophilic substitution by bromopropane.

The scanning electron microscopy images showed that Tp-MPB-COF and Tp-MPB-Br-COF have basically the same lamellar morphology [57] (Figure 2a, b). The transmission electron microscopy (TEM) and high-resolution TEM (HR-TEM) images for both COFs (Figure 2c, d) depicted ordered lattice fringes. Furthermore, the energy-dispersive X-ray spectroscopy map of Tp-MPB-Br-COF (Figure S23) revealed that Br^- was homogeneously distributed in the COF structure.

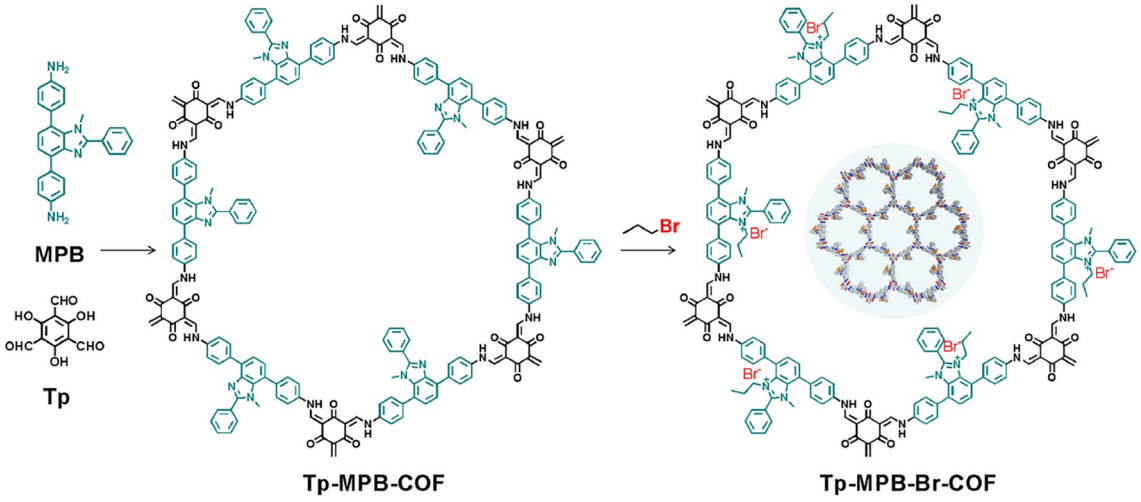

Scheme 1 Synthetic scheme of catalyst Tp-MPB-Br-COF (color online).

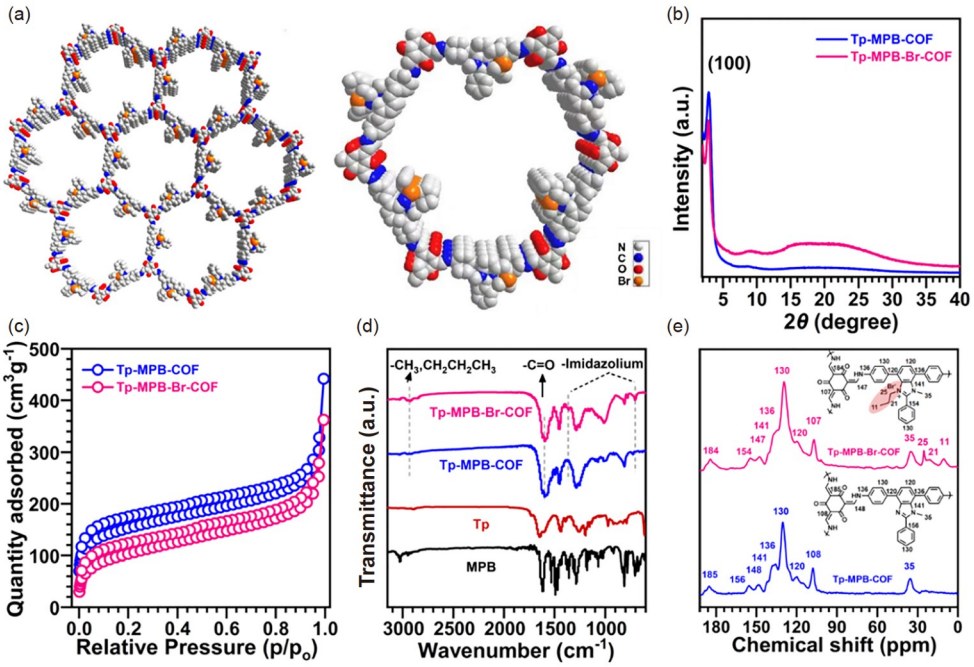

Figure 1 (a) Top view of the AA stacking mode of Tp-MPB-Br-COF. (b) XRD patterns, (c) N_2 adsorption isotherms, and (e) ^{13}C NMR spectra of Tp-MPB-COF and Tp-MPB-Br-COF. (d) FTIR spectra of MPB, Tp, Tp-MPB-COF, and Tp-MPB-Br-COF (color online).

The thermal stabilities of both COFs were also investigated using thermogravimetric analysis. The results showed that their thermal decomposition temperatures remained higher than 440 °C (Figure S24), suggesting their good thermal properties. After bromination, the thermal stability of the Tp-MPB-Br-COF reduced slightly than that of Tp-MPB-COF owing to the presence of charged Im groups [58].

The successful formation of Tp-MPB-Br-COF was investigated *via* XPS (Figure 2e–g). The N 1s spectrum of Tp-MPB-COF showed two types of nitrogen species, free secondary amine (–N–) at 400.3 eV and imidazole N (=N–) at 398.5 eV [59]. Similarly, the XPS spectrum of Tp-MPB-Br-COF revealed three nitrogen species: imidazolium N (=N^+–) at 401.6 eV, which formed owing to the bromination of the imidazolium N by bromopropane; free secondary amine (–N–) at 400.0 eV; and imidazole N (=N–) at 398.5 eV [59]. The O 1s spectrum of Tp-MPB-COF exhibited two peaks at 532.7 and 530.9 eV, attributable to the ketone and enol oxygenatoms of the keto form, respectively. The same peaks were observed in the O 1s spectrum of Tp-MPB-Br-COF (Figure 2f) [60], indicating that the keto form was not damaged after bromination. Besides, the Br 3d XPS spectra of Tp-MPB-Br-COF (Figure 2g) showed the characteristic band

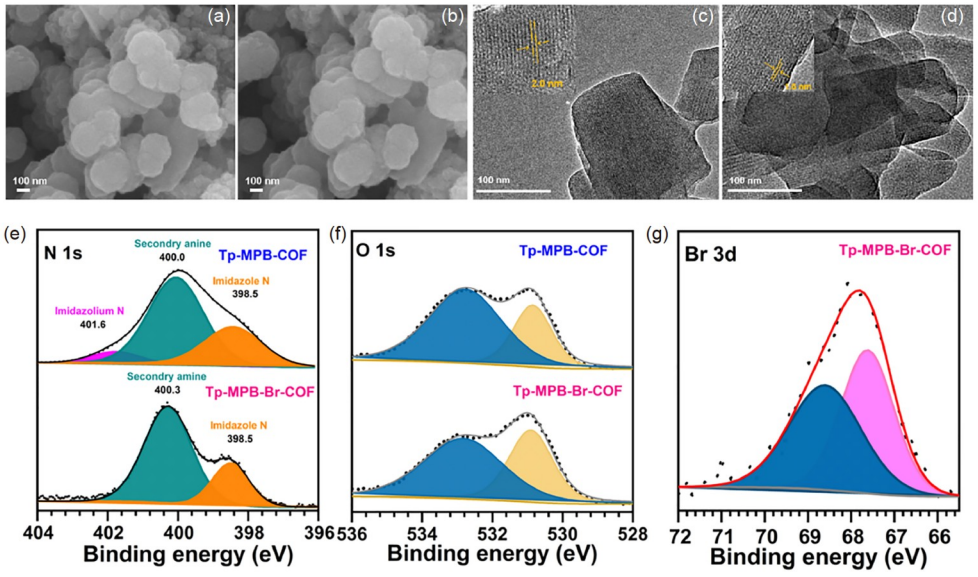

Figure 2 SEM images of (a) Tp-MPB-COF and (b) Tp-MPB-Br-COF with scale bar of 100 nm. TEM images of (c) Tp-MPB-COF and (d) Tp-MPB-Br-COF (inset: HR-TEM image and the lattice distance). High-resolution XPS spectra: (e) N 1s of Tp-MPB-Br-COF and Tp-MPB-COF. The fitted peaks correspond to imidazolium N (purple), secondary amine N (dark green), and imidazole N (orange). (f) O 1s of Tp-MPB-Br-COF and Tp-MPB-COF. The fitted peaks correspond to carbonyl O (blue) and enol O (yellow). (g) Br 3d of Tp-MPB-Br-COF. The fitted peaks correspond to Br $3d_{5/2}$ (dark blue) and Br $3d_{3/2}$ (pink) (color online).

at 68.6 eV (Br $3d_{5/2}$) and 67.6 eV (Br $3d_{3/2}$), confirming the presence of bromide anion in the Tp-MPB-Br-COF [45]. After determining the Tp-MPB-Br-COF structure, attributed to its clear pore structure, dense active sites, and excellent stability, we studied the CO_2 adsorption performance of Tp-MPB-COF and Tp-MPB-Br-COF at 273 and 298 K. As illustrated in Figure 3a, Tp-MPB-COF exhibits the highest CO_2 adsorption performance with 75.2 $cm^3\ g^{-1}$ at 273 K and 1.0 bar, while Tp-MPB-Br-COF performs poorly with 51.0 $cm^3\ g^{-1}$. The relatively decreased CO_2 adsorption capacity for the latter is mainly due to partial filling of pores and decrease in the specific surface area upon introducing bromopropane. The CO_2 uptake amount of both COFs reduced evidently at 298 K and 1.0 bar (Figure 3b). However, at 273 and 298 K, although the BET surface area of Tp-MPB-Br-COF (382.9 $m^2\ g^{-1}$) was lower than that of Tp-MPB-COF (558.6 $m^2\ g^{-1}$), the higher content of imidazolium N and Br^- in the pores of Tp-MPB-Br-COF could efficiently improve the CO_2 affinity and increase the CO_2 adsorption capacity of Tp-MPB-Br-COF at low pressure region. Briefly, the BET surface area and acid-base site content have a synergistic effect on CO_2 adsorption.

The isosteric heat of adsorption calculated according to the Clausius-Clapeyron equation was plotted against CO_2 uptake, obtaining the curves presented in Figure 3c, d. As shown in Figure 3d, the adsorption heat value of Tp-MPB-Br-COF for CO_2 was 16.51 kJ mol^{-1}, suggesting that CO_2 sorption in Tp-MPB-Br-COF is physisorption (<40 kJ mol^{-1}) rather than chemisorption [61]. The adsorption heat value of Tp-MPB-Br-COF for CO_2 decreased as the CO_2 uptake increased, indicating that the interaction between CO_2 and the adsorbent underwent a progressive decrease with CO_2 loading. Thus, Tp-MPB-Br-COF exhibits affinity with CO_2 and high CO_2 adsorption capacity (Table S4), which is conducive to the subsequent CO_2 cycloaddition reaction.

To demonstrate the catalytic performance of Tp-MPB-Br-COF with respect to the cycloaddition of CO_2, its advantages were investigated through various controlled experiments (Table S5) and the catalysis kinetics were studied using epichlorohydrin as the substrate; the catalytic yield was surprisingly 99.7% at 120 °C for 24 h. Notably, the catalyst content was only 1.5 wt% and no solvent, metal, or cocatalyst was used. Subsequently, the conversion of styrene oxide (a larger substrate) using CO_2 into styrene carbonate was selected as a typical reaction. The catalytic yield of Tp-MPB-Br-COF was twice that of Tp-MPB-COF under the same conditions (Figure 3e), indicating the key role of Tp-MPB-Br-COF in the reaction. The reaction time was extended to 48 h, and the conversion rate obtained was 98.5%. In the CO_2 cycloaddition experiment, the imidazolium N and Br^- play a more important role as catalytic active sites than the BET surface area. Compared with Tp-MPB-COF, Tp-MPB-Br-COF has more Lewis acid-base ion pairs, resulting in improved catalytic capacity. This also validates our synthesis strategy and confirms that the synergistic effect of acidity, hydrogen bonding, and Br^- precise active sites in the catalyst result in considerably improved reactivity when compared with other catalysts (Table S6).

Recovery capability is an important intrinsic characteristic of heterogeneous catalysts from the perspective of industrial

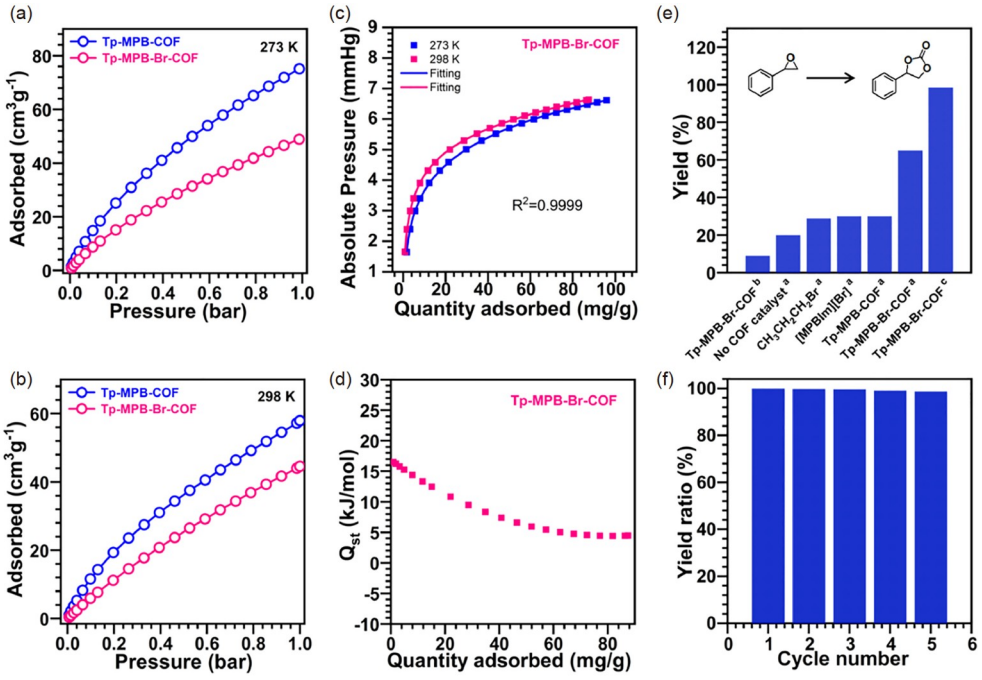

Figure 3 Adsorption isotherms of CO_2 at (a) 273 and (b) 298 K of Tp-MPB-COF and Tp-MPB-Br-COF. (c) Fitting of CO_2 adsorption equilibrium isotherms at 273 and 298 K of Tp-MPB-Br-COF. (d) Isosteric heats of adsorption for CO_2 on Tp-MPB-Br-COF. (e) Cycloaddition of CO_2 and styrene oxide under different conditions ([a] reaction condition: styrene oxide (10 mmol), COFs (20 mg, 1.5 wt%), 1 MPa CO_2, 120 °C, 24 h; [b] 1 atm CO_2; [c] 48 h). (f) Catalytic experiment of 5 cycles of CO_2 cycloaddition of Tp-MPB-Br-COF with styrene oxide (styrene oxide, 10 mmol, COFs, 1.5 wt%, 1 MPa CO_2, 120 °C, 24 h) (color online).

applications. Therefore, the cycle catalytic stability of the Tp-MPB-Br-COF was studied. As shown in Figure 3f, Tp-MPB-Br-COF undergoes five cycles of catalysis and the yields of the product remain unchanged, indicating that the catalytic ability was well maintained. Clearly, the high cyclic stability of Tp-MPB-Br-COF can be attributed to the high chemical stability of the Tp-MPB-Br-COF. Overall, Tp-MPB-Br-COF is a heterogeneous catalyst for the cycloaddition of epoxides and CO_2, which exhibits excellent catalytic performance and high stability.

The Tp-MPB-Br-COF catalyst was then recovered to test its chemical stability; there was no substantial difference in its SEM image (Figure S25), TEM image (Figure S26), FTIR (Figure S27), and solid-state ^{13}C NMR spectra (Figure S28). Moreover, the (100) peak intensity and position remained unchanged (Figure S29), indicating that C2 benzimidazolium substitution by phenyl groups effectively improved the COF chemical stability. The catalytic performance of Tp-MPB-Br-COF in CO_2 cycloaddition with more epoxides was successively investigated (Table S7). In these catalytic systems, Tp-MPB-Br-COF exhibited excellent catalytic performance and proved its superior universality.

To better understand how the imidazolium N and Br^- of the Tp-MPB-Br-COF synergistically catalyze the reaction of epoxy compounds with CO_2, a possible catalytic mechanism [52,62] was proposed (Figure 4). For Tp-MPB-Br-COF, the –OH (enol form) and –NH (keto form) groups can activate the C–O bonds of the epoxides through hydrogen bonding interactions. Moreover, the high-nucleophilicity Br^- and intermediate O^- attack the epoxy carbon atoms with low steric hindrance to open the epoxy ring. Finally, CO_2 molecules are inserted into the C–O bonds to form intermediates. The intramolecular ring-closing reaction produces cyclic carbo-

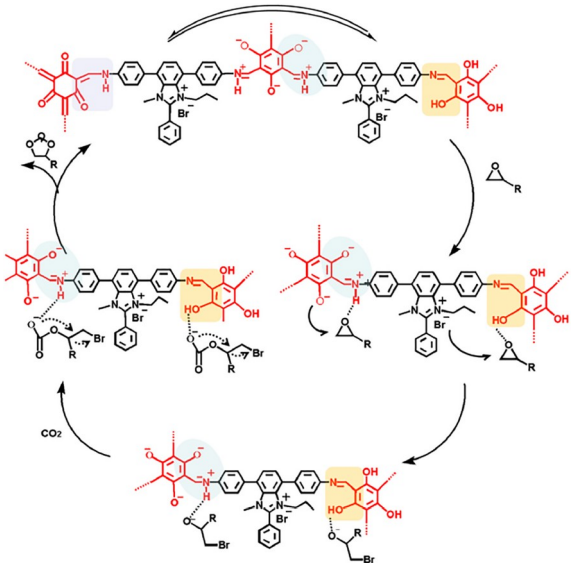

Figure 4 Scheme of possible catalytic mechanism for the reaction of epoxides and CO_2 into cyclic carbonates catalyzed by Tp-MPB-Br-COF (color online).

nate. Subsequently, the regenerated Tp-MPB-Br-COF catalyst can be used for the next catalytic reaction.

3 Conclusions

We synthesized a neutral imine COF modified by C2-phenyl-substituted benzimidazole (Tp-MPB-COF) and obtained an ionic COF for CO_2 cycloaddition. This four-in-one Tp-MPB-Br-COF catalyst has abundant multiple active sites and precise spatial locations, which improve its heterogeneous cocatalytic ability with various epoxides in CO_2 fixation under metal-, solvent- and cocatalyst-free conditions. This study will provide a new strategy for the rational design of CO_2-conversion catalysts without metals, solvents, and co-catalysts.

Acknowledgements This work was supported by the National Natural Science Foundation of China (21805173, 52273208), Shanxi Agricultural University (SXBYKY2022078, 2021BQ120), Shanxi Scholarship Council of China (2022-004), and the Natural Science Foundation of Shanxi Province (202203021211289).

Conflict of interest The authors declare no conflict of interest.

Supporting information The supporting information is available online at chem.scichina.com and link.springer.com/journal/11426. The supporting materials are published as submitted, without typesetting or editing. The responsibility for scientific accuracy and content remains entirely with the authors.

1 Luderer G, Vrontisi Z, Bertram C, Edelenbosch OY, Pietzcker RC, Rogelj J, De Boer HS, Drouet L, Emmerling J, Fricko O, Fujimori S, Havlík P, Iyer G, Keramidas K, Kitous A, Pehl M, Krey V, Riahi K, Saveyn B, Tavoni M, Van Vuuren DP, Kriegler E. *Nat Clim Change*, 2018, 8: 626–633
2 Al-Mamoori A, Krishnamurthy A, Rownaghi AA, Rezaei F. *Energy Technol*, 2017, 5: 834–849
3 Matthews HD, Gillett NP, Stott PA, Zickfeld K. *Nature*, 2009, 459: 829–832
4 Zhang Q, Yang C, Guan A, Kan M, Zheng G. *Nanoscale*, 2022, 14: 10268–10285
5 Hui W, Xu XY, Mao FF, Shi L, Wang HJ. *Sustain Energy Fuels*, 2022, 6: 3208–3219
6 Yao Q, Shi Y, Wang Y, Zhu X, Yuan D, Yao Y. *Asian J Org Chem*, 2022, 11: e202200106
7 Saptal VB, Bhanage BM. *Curr Opin Green Sustain Chem*, 2017, 3: 1–10
8 Zhao Y, Huang H, Zhu H, Zhong C. *Microporous Mesoporous Mater*, 2022, 329: 111526
9 Zhang Y, Lan X, Yan F, He X, Wang J, Ricardez-Sandoval L, Chen L, Bai G. *Green Chem*, 2022, 24: 930–940
10 Wu J, Ma S, Cui J, Yang Z, Zhang J. *Nanomaterials*, 2022, 12: 3088
11 Hao Y, Yan X, Chang T, Liu X, Kang L, Zhu Z, Panchal B, Qin S. *Sustain Energy Fuels*, 2022, 6: 121–127
12 Du YR, Yang X, Wang YF, Guan PX, Wang R, Xu BH. *Mol Catal*, 2022, 520: 112164
13 Liang S, Liu H, Jiang T, Song J, Yang G, Han B. *Chem Commun*, 2011, 47: 2131–2133
14 Ema T, Miyazaki Y, Shimonishi J, Maeda C, Hasegawa J. *J Am Chem Soc*, 2014, 136: 15270–15279
15 North M, Pasquale R. *Angew Chem Int Ed*, 2008, 48: 2946–2948
16 Dai WL, Yin SF, Guo R, Luo SL, Du X, Au CT. *Catal Lett*, 2010, 136: 35–44
17 Cao JP, Xue YS, Li NF, Gong JJ, Kang RK, Xu Y. *J Am Chem Soc*, 2019, 141: 19487–19497
18 Caló V, Nacci A, Monopoli A, Fanizzi A. *Org Lett*, 2002, 4: 2561–2563
19 Chen Y, Mu T. *Green Chem*, 2019, 21: 2544–2574
20 Roshan KR, Palissery RA, Kathalikkattil AC, Babu R, Mathai G, Lee HS, Park DW. *Catal Sci Technol*, 2016, 6: 3997–4004
21 Sun J, Cheng W, Yang Z, Wang J, Xu T, Xin J, Zhang S. *Green Chem*, 2014, 16: 3071–3078
22 Du Y, Yang H, Whiteley JM, Wan S, Jin Y, Lee S-, Zhang W. *Angew Chem Int Ed*, 2016, 55: 1737–1741
23 Baldwin LA, Crowe JW, Pyles DA, McGrier PL. *J Am Chem Soc*, 2016, 138: 15134–15137
24 Pramudya Y, Mendoza-Cortes JL. *J Am Chem Soc*, 2016, 138: 15204–15213
25 Huang N, Krishna R, Jiang D. *J Am Chem Soc*, 2015, 137: 7079–7082
26 Lin S, Diercks CS, Zhang YB, Kornienko N, Nichols EM, Zhao Y, Paris AR, Kim D, Yang P, Yaghi OM, Chang CJ. *Science*, 2015, 349: 1208–1213
27 Ding SY, Gao J, Wang Q, Zhang Y, Song WG, Su CY, Wang W. *J Am Chem Soc*, 2011, 133: 19816–19822
28 Vyas VS, Haase F, Stegbauer L, Savasci G, Podjaski F, Ochsenfeld C, Lotsch BV. *Nat Commun*, 2015, 6: 8508
29 Sun Q, Aguila B, Perman J, Nguyen N, Ma S. *J Am Chem Soc*, 2016, 138: 15790–15796
30 Wang X, Han X, Zhang J, Wu X, Liu Y, Cui Y. *J Am Chem Soc*, 2016, 138: 12332–12335
31 Sun Q, Tang Y, Aguila B, Wang S, Xiao F-, Thallapally PK, Al-Enizi AM, Nafady A, Ma S. *Angew Chem Int Ed*, 2019, 58: 8670–8675
32 Bhadra M, Kandambeth S, Sahoo MK, Addicoat M, Balaraman E, Banerjee R. *J Am Chem Soc*, 2019, 141: 6152–6156
33 Geng K, He T, Liu R, Dalapati S, Tan KT, Li Z, Tao S, Gong Y, Jiang Q, Jiang D. *Chem Rev*, 2020, 120: 8814–8933
34 Diercks C, Kalmutzki M, Yaghi O. *Molecules*, 2017, 22: 1575
35 Liu R, Tan KT, Gong Y, Chen Y, Li Z, Xie S, He T, Lu Z, Yang H, Jiang D. *Chem Soc Rev*, 2021, 50: 120–242
36 Lohse MS, Bein T. *Adv Funct Mater*, 2018, 28: 1705553
37 Liang RR, Jiang SY, A RH, Zhao X. *Chem Soc Rev*, 2020, 49: 3920–3951
38 Li J, Wang J, Wu Z, Tao S, Jiang D. *Angew Chem Int Ed*, 2021, 60: 12918–12923
39 Wu Z, He Y, Liu L, Wang J, Xu Q, Zhang XM, Li J. *ACS Appl Mater Interfaces*, 2022, 14: 43861–43867
40 Yang X, Jin Y, Yu B, Gong L, Liu W, Liu X, Chen X, Wang K, Jiang J. *Sci China Chem*, 2022, 65: 1291–1298
41 Liu H, Yan X, Chen W, Xie Z, Li S, Chen W, Zhang T, Xing G, Chen L. *Sci China Chem*, 2021, 64: 827–833
42 Wu Z, Huang X, Li X, Hai G, Li B, Wang G. *Sci China Chem*, 2021, 64: 1964–1969
43 Tong Y, Cheng R, Dong H, Liu B. *J Porous Mater*, 2022, 29: 1253–1263
44 Zhang Y, Yang DH, Qiao S, Han BH. *Langmuir*, 2021, 37: 10330–10339
45 Li Y, Zhang J, Zuo K, Li Z, Wang Y, Hu H, Zeng C, Xu H, Wang B, Gao Y. *Catalysts*, 2021, 11: 1133
46 Li Y, Song X, Zhang G, Chen W, Wang L, Liu Y, Chen L. *Sci China Mater*, 2021, 65: 1377–1382
47 Peng J, Deng Y. *New J Chem*, 2001, 25: 639–641
48 Su Q, Qi Y, Yao X, Cheng W, Dong L, Chen S, Zhang S. *Green Chem*, 2018, 20: 3232–3241
49 Cui C, Sa R, Hong Z, Zhong H, Wang R. *ChemSusChem*, 2020, 13: 180–187
50 Ding LG, Yao BJ, Jiang WL, Li JT, Fu QJ, Li YA, Liu ZH, Ma JP, Dong YB. *Inorg Chem*, 2017, 56: 2337–2344

51 Yan Q, Liang H, Wang S, Hu H, Su X, Xiao S, Xu H, Jing X, Lu F, Gao Y. *Molecules*, 2022, 27: 6204
52 Du YR, Ding GR, Wang YF, Xu BH, Zhang SJ. *Green Chem*, 2021, 23: 2411–2419
53 Luo R, Liu X, Chen M, Liu B, Fang Y. *ChemSusChem*, 2022, 13: 3945–3966
54 Yang Y, Chen K, Liu X, Chen M, Xu W, Liu B, Ji H, Fang Y. *J Mater Chem A*, 2021, 9: 20941–20956
55 Wang KY, Yang Q, Chung TS, Rajagopalan R. *Chem Eng Sci*, 2009, 64: 1577–1584
56 Thomas OD, Soo KJWY, Peckham TJ, Kulkarni MP, Holdcroft S. *J Am Chem Soc*, 2012, 134: 10753–10756
57 He C, Si D, Huang Y, Cao R. *Angew Chem Int Ed*, 2022, 61: e202207478
58 Kang DW, Kang M, Yun H, Park H, Hong CS. *Adv Funct Mater*, 2021, 31: 2100083
59 Lin X, Varcoe JR, Poynton SD, Liang X, Ong AL, Ran J, Li Y, Xu T. *J Mater Chem A*, 2013, 1: 7262–7269
60 Ito E, Oji H, Araki T, Oichi K, Ishii H, Ouchi Y, Ohta T, Kosugi N, Maruyama Y, Naito T, Inabe T, Seki K. *J Am Chem Soc*, 1997, 119: 6336–6344
61 Liu TT, Xu R, Yi JD, Liang J, Wang XS, Shi PC, Huang YB, Cao R. *ChemCatChem*, 2018, 10: 2036–2040
62 Huang K, Zhang JY, Liu F, Dai S. *ACS Catal*, 2018, 8: 9079–9102